Journal of Marine Science and Application (2025) 24: 1164-1173
https://doi.org/10.1007/s11804-025-00612-9

RESEARCH ARTICLE

Impact of Blade Pitch Angle on the Turbine Performance of a Vertical Axis Current Turbine

Johan Forslund[1], Victor Mendoza[1,2] and Anders Goude[1]

Received: 13 May 2024 / Accepted: 21 October 2024

Abstract
Marine current energy conversion with turbines is a growing field of interest owing to its high energy density and predictability. For wind energy, three-bladed horizontal-axis turbines are the most common because of their high power capture. Forces on blades are considerably higher in marine currents, presenting challenges to turbine design. Current research focuses on blade optimization and the selection of reliable transmission systems, and data from experiments conducted in natural environments are lacking. This paper focuses on a five-bladed vertical axis marine current turbine with a direct drive generator especially designed for low rotational speed and presents data from real-world experiments and 3D simulation models. The paper specifically investigates the influence of blade pitch angle on power capture. Experiments have been conducted at 1.42 m/s with a turbine in a river for blade pitch angles of 0° and +3° (the angle is defined as the leading edge of the blade rotating outward, perpendicular to, and opposite of the turbine axis). Two numerical 3D models, namely a vortex model and an actuator line model, have been used to simulate the turbine under the same conditions (1.42 m/s and 0°, +3°). The experimental and simulation results show that a 0° pitch angle gives a higher power capture power than a +3° pitch angle. In addition, simulation models were used to simulate the performance for an extended range at pitch angles of −3° to +3°, a fixed tip-speed ratio, and a step size of 1°. The simulations show that +1° gives the highest power coefficient and increases the average power capture by up to 0.6%. The performance of vertical axis marine current turbines can be improved by increasing the pitch angle to 1° in the positive direction. By contrast, a negative pitch angle can increase the average power capture of wind turbines.

Keywords Marine current energy converter; Vertical axis turbine; Pitch angle; Actuator line model (ALM); Vortex; Permanent magnet synchronous generator

1 Introduction

The conversion of waves and ocean currents is investigated using different concepts and devices floating on the surface, suspended between the surface and the bottom, or placed directly on the bottom (Day et al., 2015). For marine current energy, turbine configurations and nonturbine systems are considered in the conversion of energy in free-flowing water (Khan et al., 2009; Uihlein and Magagna, 2016; Zhou et al., 2014). In turbine-based designs, the horizontal axis comprises the majority of solutions and its higher power capture compared with that of vertical axis turbines is the major advantage. However, marine converters using a vertical axis current turbine (VACT) is a field of growing interest. The advantages of vertical axis turbines are as follows:

• The turbine absorbs power from incoming water flowing perpendicular to the turbine axis (omnidirectional). Thus, it does not need a yawing system.

• The manufacturing costs of the blades are lower because no twist occurs along the blade.

• Installation and maintenance costs are reduced because the generator and gearbox are placed at the bottom of the converter.

• The center of gravity is low.

• The blades have no cyclic gravitational loads.

Article Highlights

- The article presents the performance of a vertical axis marine current turbine's response to blade pitch angle variation. Experimental data at different pitch angles are lacking.
- The work presents data from simulations and data collected from a prototype turbine placed in a river. The work uses two validated advanced numerical 3D models that confirm the presented experimental results.
- The results are new compared with turbine design for vertical axis wind turbines. Specifically, the results suggest that the pitch angle should be changed in the opposite direction from what is used in wind turbines for the optimization of power outtake.

✉ Johan Forslund
johan.forslund@angstrom.uu.se

[1] Department of Electrical Engineering, Uppsala University, Uppsala 75310, Sweden

[2] Hexicon, Hexicon AB, Östra Järnvägsgatan 27, Stockholm 11120, Sweden

When testing the performance of the turbine in a real-world setting, the influence of boundary conditions should be considered. In a tank or a cavitation tunnel, the boundary exerts a considerable impact and creates blockage effects. For example, the difference in power capture from a turbine between tank testing and open flow can reach up to 18% (Bahaj et al., 2006) and theoretically up to 100% (Garrett and Cummins, 2007). If a turbine is placed in an extremely wide channel or the ocean, performance should be tested under similar conditions. How the characteristics of turbine performance depend on hydrodynamic design is currently explored. One way of increasing the power coefficient of a vertical axis turbine is to identify the optimal blade pitch angle. However, experimental tests for marine current turbines are lacking, although an initial test in 1981 by Sandia National Laboratories (Klimas and Worstell, 1981) for a small-scale vertical axis wind turbine (VAWT) provides a reference for most simulation models; the test showed that the power capture can be up to 50% higher than the lowest value at pitch angles from 3° to −7°. Notable results from research into VAWTs might provide an indicator for hydrodynamic performance.

- −2° was the optimum for a three-bladed Darrieus turbine (Klimas and Worstell, 1981), experimentally investigated for angles −7° to 3°.
- −7.8° was the optimum for a high solidity 3-bladed H-rotor (Fiedler, 2009) with $\lambda_{optimal}$ of 1.6, experimentally investigated for angles −7.8° to 7.8°.
- −6° was the optimum for a three-bladed H-rotor (Armstrong et al., 2012) with $\lambda_{optimal}$ of 1.6, experimentally investigated for angles −12° to 12°.
- −6° was the optimum for a three-bladed H-rotor (Kaya et al., 2022) with $\lambda_{optimal}$ of 6.5, investigated with numerical simulations from −6° to 2°.
- −2° was the optimum for a three-bladed H-rotor (Rezaeiha et al., 2017) with $\lambda_{optimal}$ of 4.0, investigated with numerical simulations from −7° to 3°.

The optimal angle is dependent on turbine type, and most turbine types for wind power utilize three blades. Notably, water has a density of roughly 830 times that of air and a considerably lower flow speed. Thus, current turbines not only have a different Reynolds number from wind turbines but also have lower optimal tip-speed ratios. These characteristics lower the rotational speed for the optimal tip-speed ratio and, in turn, produce large forces and torque on turbine blades. For each blade, a position in each revolution of a turbine produces maximum torque, and for current turbines, this difference is more pronounced. A three-bladed turbine thus produces three peaks of torque for each revolution. To reduce the oscillations of torque, the number of blades can be increased, but the amount of material needed for production increases. A comparison of three- and five-bladed VAWTs (Li et al., 2015) shows that by increasing the number of blades, normal forces per blade can be reduced by a factor of two; the maximum power capture and optimal tip-speed ratio are slightly reduced. Similar results are achieved in another study comparing two-, three-, and four-bladed VAWTs (Delafin et al., 2016).

Research on real-world environments for VACTs has gaps, for example, the impact of pitch angle on power capture. The first experiment on power capture as a function of tip-speed ratio was performed by Kiho et al. (1996), who used a Darrieus type three-bladed current turbine. However, the field has not drawn considerable attention from researchers focusing on solar or wind power. The ability to change the pitch during operation would be an efficient way of optimizing the power capture of a turbine and has been studied for wind turbines (Miau et al., 2012; Paraschivoiu et al., 2009). The yearly energy yield can be increased to up to 30% for a VAWT (Paraschivoiu et al., 2009) and low tip-speed ratio turbines. This solution increases the complexity of a design and should be considered for VAWTs, given that wind turbines are relatively easy to maintain. However, whether the cost-benefit of VACTs is more favorable than that of a fixed pitch turbine with an optimized pitch angle is unclear.

A comparison between tidal turbines and fixed pitch and active pitching turbines demonstrated considerable impact on pitch angle at a low optimal tip-speed ratio. Mannion et al. (2019) used a 2D CFD model and experimental data from a 1:20 scaled test in a flume of two turbines with a bluff body between to determine whether the power factor could be increased from 0.21 to 0.37 through active pitching at a tip-speed ratio of 0.45. The experimental results showed that the efficiency of the implemented active pitching can be easily affected and the complexity of the design increases. Further, Chen et al. (2018) used a 2D CFD numerical model to increase the power factor through active sinusoidal pitching at a tip-speed ratio of 1.45. 2D models overestimate power capture but greatly reduce computation time. In this study, 3D models will be used to increase accuracy, and experimental results from field tests in a river for a turbine designed for a tip-speed ratio of 3.1 will be presented. Given that the low tip-speed ratios of turbines benefit from an optimized pitch angle, the increase in power capture is expected to be lower than the increases reported by Mannion et al. (2019) and Chen et al. (2018).

Performing experimental tests on a turbine in a real-world setting is difficult and expensive (Gu et al., 2024), and thus, most VACT studies are made by using simulations and testing or cavitation tunnel. Most of the research for current turbines has surrounded optimizing blade design and selecting a transmission system (Gu et al., 2024). This paper aims to fill the gap by presenting experimental data from a turbine in a river, extending numerical simulations to 3D, and exploring the influence of blade pitch angle on the power performance of a five-bladed VACT.

1.1 Marine current power project at uppsala university

The Marine Current Power Project at Uppsala University is investigating the possibility of using a VACT to extract power from slow-moving marine currents, as shown in Figure 1. The device is rated at 7.5 kW and has five fixed pitch blades. The turbine is connected in direct drive to a permanent magnet synchronous generator (PMSG); that is, no gearbox is used . A prototype generator and turbine has been deployed in the Dal River in Söderfors, Sweden (Lundin et al., 2013), where the water speeds are usually 0.4–1.5 m/s (Yuen et al., 2011).

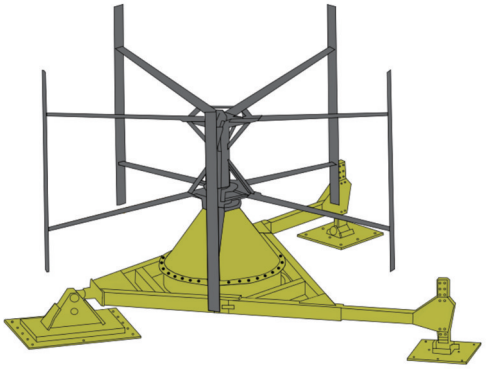

Figure 1 Marine current converter using a vertical axis turbine at Uppsala University

2 Turbine

The power in free-flowing water (P_{flow}) that passes through a turbine with cross-section A is described by

$$P_{\text{flow}} = \frac{1}{2} A\rho V^3 \tag{1}$$

where V is the water speed passing by the cross-section of the turbine and ρ is the density of water. The power coefficient C_{P} is the fraction of power delivered to the generator ($P_{\text{generator}}$) from the turbine and is defined as

$$C_{\text{P}} = \frac{P_{\text{generator}}}{P_{\text{flow}}} \tag{2}$$

The power coefficient is a function of the tip-speed ratio (λ), which is the ratio of blade speed to undisturbed water speed and is defined as

$$\lambda = \frac{\Omega r}{V} \tag{3}$$

where Ω is the rotational speed of the turbine (rad/s), and r is the turbine radius. The maximum power capture for the turbine is $C_{\text{P, max}} = 0.26$ at $\lambda_{\text{optimal}} = 3.1$ (Lundin et al., 2016). Estimation of power extracted from the turbine assumes losses of 180 N·m as iron, seal, and frictional losses. The losses have been validated to be closer to 350 N·m (Forslund et al., 2018).

The vertical axis turbine has five blades with fixed pitch and NACA 0021 profile, is 3.5 m high, and has a radius of 2.94 m and chord length of 0.18 m. The design for attaching the blades to the struts allows for the selection of a pitch angle between 0° to +3°. Each blade is attached to two struts, using screws. One of the holes on the blades is larger than the screws, allowing for the changing of the angle. The positive direction of the pitch angle γ is defined as the leading edge of the blade rotating outward, as shown in Figure 2. Note that this angle is sometimes defined in the opposite direction. The blades of the first turbine prototype were mounted at 0°, and those of the second prototype were mounted at +3°. The turbine parameters are provided in Table 1.

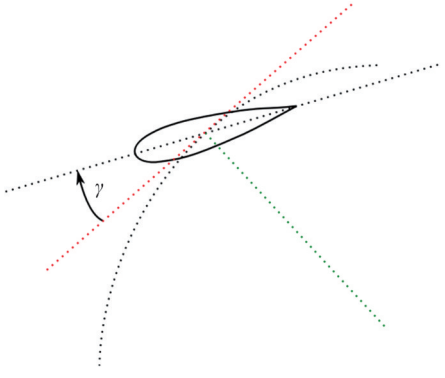

Figure 2 Definition of the pitch angle γ for the VACT

3 Söderfors experimental station

The marine current converter consists of a turbine and generator on the bottom of the river and is connected via power cables to a control and measurement cabin on shore. The converter is placed 800 m downstream of a

Table 1 Söderfors turbine prototype specifications at rated speed

Converter rating (kW)	Estimated iron, seal, and frictional losses (N·m)	$C_{\text{P, max}}$	Rated water speed (m/s)	Rated rotational speed (r/min)	Number of blades	Blade material	Blade pitch angle	Blade profile	Turbine radius (m)	Turbine height (m)	Chord length (m)
7.5	350	0.26 at $\lambda = 3.1$	1.35	15	5	Carbon fiber	Fixed at 0° or 3°	NACA 0021	2.94	3.5	0.18

commercial hydropower plant at a depth of 7 m (Figure 3). The experimental station has been described by Lundin et al. (2013), Yuen et al. (2011), and Grabbe et al. (2009), and the generator has been described by Grabbe et al. (2013). In the river, two acoustic Doppler current profilers (ADCPs) are installed to register the water speed.

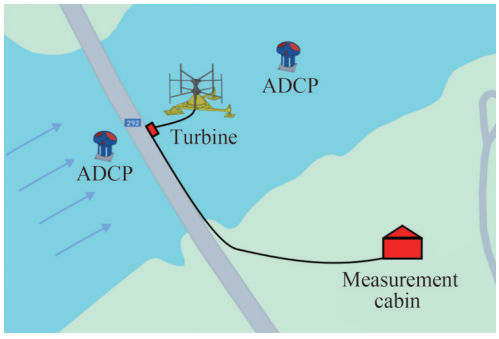

Figure 3 Turbine and water speed measurement devices (ADCPs) installed in the Dal River (Dalälven) and the onshore measurement cabin at the experimental site in Söderfors, Sweden

3.1 Generator and electrical system

The prototype generator is a directly driven PMSG, and the rated operation of the converter system is at a water speed of 1.35 m/s. The purpose of using a direct-drive configuration is to reduce maintenance related to a gearbox, and the low water speed results in the low rotational speed of the turbine and maintains the maximum CP. The configuration does not allow the generator to have a rotational speed different from that of the turbine, increasing the output voltage and reducing copper losses. Thus, the generator should be efficient at rated turbine rotation speeds of 5–16.7 r/min, which correspond to electrical frequencies of 4.7–15.6 Hz for the generator. The generator has an experimentally verified efficiency of at least 80% for all rotational speeds (Grabbe et al., 2013). The specifications of the generator can be found in Table 2, and a detailed description of the generator design, construction, and testing has been provided by Grabbe et al. (2013). The generator is connected to the measurement cabin on shore by a three-phase power cable (approximately 150 m long) with a resistance of 0.08 Ω/phase. The generator, and therefore the turbine, is controlled using CompactRIO and LabView. During operation, the generator is connected to a fixed resistive Wye-connected AC load. The rotational speed is calculated using Hall sensors inside the generator. The control and measurement system is fully described by Yuen et al. (2013).

3.2 Water speed measurements using ADCPs

The water speed is logged by an ADCP placed approximately 15 m upstream of the turbine, and the river bed depth of the ADCP is assumed to be the same as that of the turbine. The device is a Workhorse Sentinel 1 200 Hz with an accuracy of 0.3% for water speed. Measurements are obtained every 3.6 s, and the velocity profile from 1 m above the bottom of the river to 1 m below the surface is determined. The logged data provide the cubic mean value of the vertical speed profile. The speed of the water at the measurement point of the ADCP is assumed to be constant until the water reaches the turbine.

4 Simulation models

The effect of blade pitch angle on turbine performance will be explored on the basis of experimental results and two simulation models outlined in this section. The Vortex and Actuator Line models have been validated for a 12 kW VAWT (Mendoza and Goude, 2020). The wind turbine selected for validation is a straight-bladed Darrieus turbine and features three blades with a fixed pitch of +2°. The simulated normal forces of the turbine are validated using the force measurements obtained using load cells (Rossander et al., 2015; Dyachuk et al., 2015a). The models presented demonstrate the capability to replicate normal forces on a blade of a VAWT under various operational conditions in an open site. A satisfactory agreement with experimental data is observed in terms of the trends, magnitudes, and amplitudes of the predicted forces. The models can identify the region for optimal tip-speed ratio operation (yielding higher C_p) and the maximum and minimum loads on blades within one revolution. Both models provide a qualitatively accurate representation of the turbine power curve, although discrepancies arise in the representation of peak and drop forces in the first and second halves of the revolution, respectively (with the exception of the actuator line model (ALM) for high tip-speed ratios). These discrepancies underscore the considerable influence of the method for obtaining the angle of attack and the input data for force coefficients. A decrease in accuracy is noticeable in cases with high tip-speed ratios, where a force drop occurs in the second half of the revolution.

4.1 Actuator line model (ALM)

The ALM, developed by Sørensen and Shen (1999), is

Table 2 Generator specifications at nominal operation

Rated electrical frequency (Hz)	Poles	Rated line-to-line root mean square (RMS) voltage (V)	Rated stator current (A)	Power rating (kW)	Stator phase resistance (Ω)	Armature inductance (mH)
14	112	138	31	7.5	0.335	3.5

based on the classic blade element method and serves as a three-dimensional unsteady aerodynamic model for characterizing flow generated by turbine rotors. This approach partitions a blade into n elements behaving as two-dimensional airfoils, and forces are determined using a dynamic stall model (DSM) based on empirical values.

The implementation of the ALM necessitates lift and drag coefficient values for different angles of attack and Reynolds numbers characteristic of blade motion. The relative speed and angle of relative wind (V_{rel} and φ, respectively) are calculated on the basis of the geometric relationship between the tangential speed of the blade (V_{blade}) and incoming flow (V_{in}) (typically smaller than the freestream speed V_{∞}):

$$\overrightarrow{V_{rel}} = \overrightarrow{V_{in}} - \overrightarrow{V_{blade}} \tag{4}$$

Blade speed V_{blade} is represented as Ωr, where Ω is the angular speed of the rotor and r is the radius of the turbine.

The relative wind angle ($\varphi = \alpha + \gamma$) is defined by the sum of the angle of attack and the blade pitch angle (γ). An illustration depicting the velocities and forces involved in a blade cross-section is presented in Figure 4. θ is the azimuthal angle. Inflow speed is determined by averaging the speed from a defined number of samples around an element and is symmetrically distributed in the profile plane at the quarter chord position. A sensitivity study regarding the sampling radius and number of samples reveals that a suitable combination is 2ϵ and 20, respectively. The variable ϵ is the smoothing width parameter of the Gaussian function used for force projection, and V_{cell} denotes the volume of the cell.

$$\epsilon = \max\left[\frac{c}{4}, 4\sqrt[3]{V_{cell}}, \frac{cC_D}{2}\right] \tag{5}$$

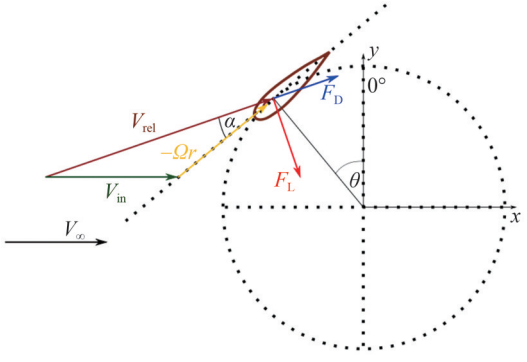

Figure 4 Illustration of speed vectors and forces acting at the cross-section of the blade in a VAWT

where c is the chord length and C_D is the drag force coefficient. Once the V_{rel} and α are calculated, the lift and drag forces per spanwise length unit are obtained through the expressions

$$f_L = \frac{1}{2}\rho c C_L \left|V_{rel}\right|^2 \tag{6}$$

and

$$f_D = \frac{1}{2}\rho c C_D \left|V_{rel}\right|^2 \tag{7}$$

where C_L is the lift force coefficient. These coefficients are functions of the local angle of attack and the Reynolds number and are linearly interpolated from a table per local α. Subsequently, a DSM combined with the blade element approach determines body forces acting on the blade. The lift component is perpendicular to the relative speed V_{rel} and the blade span direction, whereas the drag component shares the same direction as V_{rel}. The same methodology is applied to the calculation of forces on the shaft (tower) and struts. After the calculation of all actuator element forces, they are integrated as body source forces per unit density into the momentum conservation equation.

The ALM has been implemented using the *turbinesFoam* library developed by Bachant and Wosnik (2015), Bachant et al. (2016a, 2016b). This implementation has been previously validated (Mendoza et al., 2016; Mendoza and Goude, 2017; Mendoza et al., 2018a; Mendoza, 2018b) under various turbine operating conditions in wind tunnels and open sites. A concise explanation of the ALM is provided in this section. The ALM and DSM are comprehensively documented by Bachant et al. (2016a) and Dyachuk (2015b), respectively.

4.2 Hydrodynamic vortex model

The hydrodynamic vortex model operates on a principle similar to that of the ALM, involving the calculation of the velocity field to derive the relative flow velocity and angle of attack. This angle is utilized by a DSM to compute blade forces and subsequently integrated into the flow field. The same DSM employed in the ALM is utilized here.

The vortex method is predicated on discretizing the vorticity field rather than the velocity field. It employs a vortex filament method, where vorticity elements are advected with the flow velocity, which is determined by solving Biot-Savart's law at each time step. The released vortex strength is computed as the change in circulation around the blade and derived from the lift force with Kutta-Joukowski's lift theorem, neglecting the effect of drag forces. The tip vortex strength is automatically derived by enforcing the divergence-free characteristic of a vorticity field.

A notable distinction between the ALM and vortex method implementations lies in the calculation of the angle of attack. Instead of sampling velocity at the quarter chord position, a potential flow solution is utilized. Owing to the extensive number of discretization elements required to model a blade surface, blades are modeled as flat surfaces

with a vortex lattice. The utilization of a vortex lattice in resolving the no-penetration boundary condition of the flat surface directly generates tip vortices, eliminating the need for additional tip correction models as required in the ALM.

Another important difference between vortex filament methods and traditional finite volume method solvers is that the filament method retains the connectivity of the vortex elements. This feature assures a divergence-free vorticity field and limits artificial diffusion during convection, but vortex stretching results in extremely long filaments and considerable discretization errors when the wake breaks down into a fully turbulent state. As these errors occur early in the presence of large thrust forces generation by fast turbine rotation, the model is suitable for low rotational speeds.

Support arms are incorporated as additional blade elements and treated in the same manner as blades during lift generation.

The vortex method employs 90 steps per turbine revolution, and simulations are conducted for 25 turbine revolutions. The blades are modeled using 30 spanwise segments, and 15 segments are added for each support arm.

5 Design of experiments and simulations

This study aims to showcase simulation and experimental data and show how a selected blade pitch angle affects the power capture of a turbine. First, experimental results of the turbine operating without an electrical load are presented. The free-spin rotational speed and tip-speed ratio (λ) of the turbine are determined while it is spinning freely. Second, experimental data from when the generator is connected to AC loads of varying electrical resistance for a fixed water speed are presented, and λ versus C_P-curves and the calculated optimal tip-speed ratio, λ_{opt}, for blade pitch angles of 0° and +3°. The turbine design is made to be robust, and the need for maintenance is reduced by minimizing the number of moving parts. Given that maintenance issues with variable pitch turbines arise from mechanical parts for adjusting the pitch, this turbine is a fixed pitch turbine. However, the angle can be adjusted by divers without removing the turbine from the river. Owing to the difficulties in working submerged and the high costs associated with extracting and redeploying turbines, the only reasonable solution is the adjustment of the angle to the maximum or minimum value of a certain range by a diver. This range was selected to include the angle that resulted in the maximum power capture in the simulations, which is between 0° and +3°. The third part of the investigation uses the conditions of previously described experiments as inputs for both simulation models and extends the investigated range of pitch angles to −3°–3° at a step size of 1°. On the basis of the simulated data, $C_P(\lambda_{opt})$ -curves are compared with experimental data. In the last part, the angle of attack as a function of azimuthal angle during a full revolution of the turbine is presented.

5.1 Free-spin operation experiment setup

The turbine was operated without load for 30 min at water speeds below and above the turbine rating of 1.35 m/s. The tip-speed ratio for each experiment is calculated from the average of the measured water speed and the average of the measured rotational speed of the turbine. Eight measurements were made for a pitch angle of 0° at water speeds from 0.99 m/s to 1.53 m/s. A total of 15 measurements were made for a pitch angle of 3° at water speeds from 0.88 m/s to 1.61 m/s.

5.2 AC-load experiment setup

Data were collected with electrical AC-loads connected to the generator. Each experiment was carried out for 30 min at a water speed of 1.42 m/s. and the resistive loads ranged from 1.7 Ω to 10 Ω. The loads were selected to cover operation in tip-speed ratios below, near, and over the expected λ_{opt} = 3.1. At a pitch angle of 0°, four experiments were conducted at tip-speed ratios of 2.95, 3.20, 3.37, and 3.51. For a pitch angle of +3°, six experiments were conducted at tip-speed ratios of 3.03, 3.12, 3.41, 3.65, 3.77, and 3.87. The power extracted is calculated as the average value of the sum of the power in the load, power losses in the transmission line and generator windings, and the iron, seal, and frictional losses. The iron, seal, and frictional losses have been validated to be linearly dependent on rotational speed as 350 ω (Forslund et al., 2018). The power absorbed by the turbine was estimated using Equation (1) and the measured water speed. The power coefficient for each water speed was calculated using Equation (2). The tip-speed ratio of each experiment was calculated using Equation (3), along with the average measured water speed and rotational speed.

5.3 Simulations setup

Turbine operation was simulated at a rated speed of 1.35 m/s with both simulation models. In addition to the blade pitch angles of 0° and +3° used for the experiments, a pitch angle of −3° was simulated. In each simulation, the turbine had 25 revolutions, and the average C_P was calculated as the average value of the last revolution. The C_P curve was simulated for tip-speed ratios of 2–4.4. The tip-speed ratio step size for the vortex model was 0.1 but was reduced to 0.2 for the ALM because it is more computationally demanding. The effect of pitch angle on power capture was investigated in detail by simulating C_P versus pitch angle at a fixed tip-speed ratio of 3.4 and pitch angles ranging from −3° to +3° at 1° intervals.

6 Experimental and simulation results

6.1 Experimental results of the turbine during free-spin operations

Rotational speeds and tip-speed ratios during free-spin operations are shown in Figures 5 and 6. At 0° pitch angle, the turbine operates at a higher rotational speed, except at low and and high speeds where it is in the same range as the turbine with +3° pitch. The drag losses in the turbine are lower at 0° pitch angle than at +3°, which should result in a high power capture.

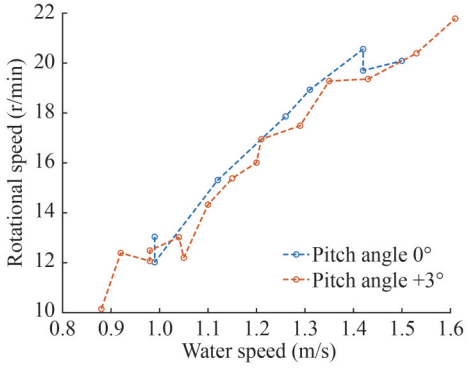

Figure 5 Experimentally measured rotational speed at free-spin for pitch angles +3° and 0°

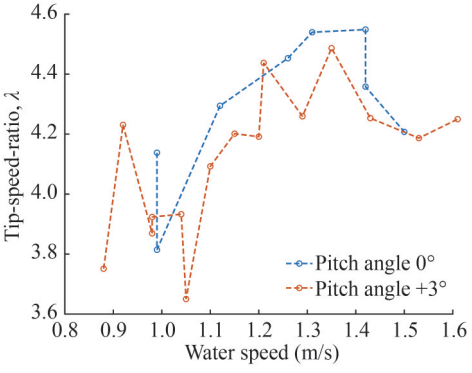

Figure 6 Experimentally measured tip-speed ratio during free-spin operations for pitch angles +3° and 0°

6.2 Experimentally measured and simulated λ_{opt}

The tip-speed ratios with the highest C_P -values (λ_{opt}) for each pitch angle are listed in Table 3. The ALM and vortex models predict a higher λ_{opt} for the lowest investigated pitch angle. However, the experiments show a slightly higher λ_{opt} for +3° pitch angle compared with the 0° pitch angle, but the difference is quite small.

6.3 Experimentally measured and simulated $C_P(\lambda)$ -curves

The C_P curves for tip-speed ratios of 2–4.4 can be seen in Figure 7. The experiment shows a reduction in C_P at the blade pitch angle increases. The highest measured C_P for both angles decreases by 25.7% at a blade pitch of +3°. The simulations predict different results. The ALM simulation shows a reduction of 5.1% for the 3° pitch angle. A slight increase at the highest C_P is predicted (2.6%), but the vortex simulation shows a reduction of 5.1% at 3° compared to 0°. Note that the ALM simulation shows a higher C_P for 0° at a tip-speed ratio of 2.8 or higher, and a higher C_P for +3° (below 2.8). For the vortex simulation, the 0° pitch always gives a C_P value higher than that at +3° pitch angle.

Table 3 Generator specifications at nominal operation

Pitch angle (°)	Vortex λ_{opt}	ALM λ_{opt}	Experiment λ_{opt}
−3	4.0	3.0	-
0	3.6	2.8	2.9
+3	3.5	2.6	3.0

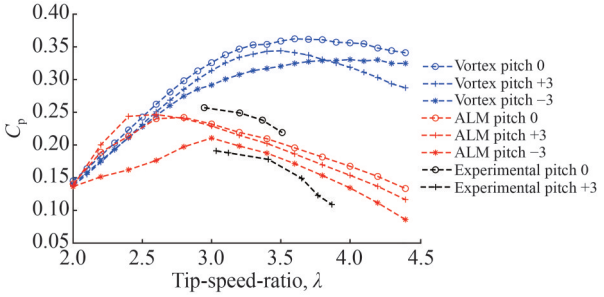

Figure 7 Simulated and experimentally measured C_P-curves at three different pitch angles for tip-speed ratios of 2–4.4

To investigate the impact of a negative pitch angle on power capture, the simulations include a pitch angle of −3° for tip-speed ratios from 2.0 to 4.4, which were not covered by the experiments. The vortex simulation predicts a reduction of maximum power capture of 8.6%, but the ALM simulation predicts an increase of 2.1%. The ALM model has a stronger agreement with experimental data in comparison with the vortex model.

6.4 Power capture as a function of pitch angle, $C_P(\gamma)$

The experimentally measured and simulated C_P versus λ curves (discussed in Section 6.3) shows that the 0° pitch angle has the highest C_P among the three investigated angles in the experiment and vortex simulation, but the ALM simulation predicts a higher C_P for the −3° pitch angle. The power capture curve at a tip-speed ratio of 3.4 for pitch angles of −3° to +3° was simulated with a step size of 1°. The objective was to identify the pitch angle with the highest power capture.

Figure 8 shows how the power coefficient depends on

the pitch angle. The experiments only have two measurement points, and thus, validating the simulated values is difficult. In addition, a considerable difference in the predicted maximum power coefficient was found. However, the purpose of the study is to investigate the impact of pitch angle on power capture, and the trend of power capture over pitch angles is essential.

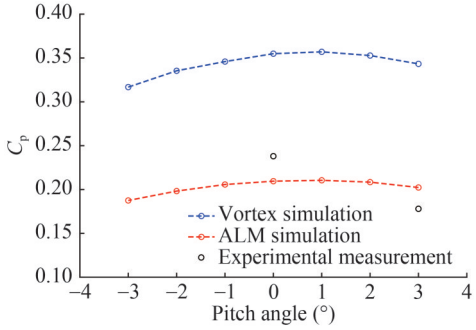

Figure 8 Simulated and experimentally measured average C_p at a tip-speed ratio of 3.4 as a function of pitch angle with a simulated step size of 1°

Both simulation models predict that the highest average C_p of the turbine is achieved at a pitch angle of +1°, and C_p increases by 0.6% for ALM and 0.5% for vortex relative to the value obtained at 0°. In fact, the results show that in a vertical axis marine current turbine, performance could be improved by increasing the pitch angle in the positive direction by one degree. This result is inconsistent with the results of studies on wind turbines, where a negative pitch angle can increase the average power capture.

6.5 Simulations of angle of attack as a function of azimuthal angle

The results presented in Sections 6.3 and 6.4 focus on the impact of pitch angle on power capture, but the difference in predicted power capture among the simulations was not addressed. The difference is clearly seen in Figure 8, where the vortex model predicts a power capture of 70% higher than the ALM model. A part of the differences can be explained by variations in angles of attack in a single turbine revolution simulated by the two models.

Figure 9 shows the angle of attack as a function of the azimuthal angle for one revolution for both simulation models at a pitch angle of 0° and tip-speed ratio of 3.4. The results are summarized in Table 4.

The ALM model predicts maximum and minimum values 0.59°–1.06° higher than those predicted by the vortex model. This difference in the projected angle of attack in the tangential direction should have a large impact on the projected tangential forces, which in turn produces a considerable difference in projected power capture, explaining the large difference observed in Figure 8. Notably, hydrodynamics is extremely sensitive because the angle of attack is within the dynamic stall regime. The large difference in the high tip-speed ratio is likely because of the discretization errors in the vortex filament method due to extensive vortex stretching.

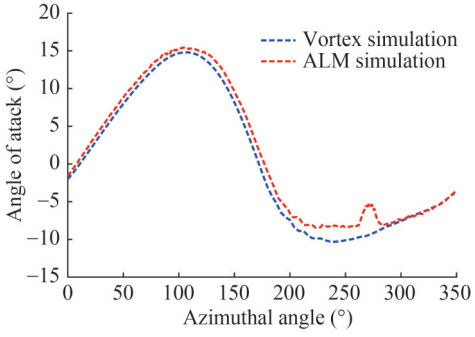

Figure 9 Simulated values for azimuthal angle vs. angle of attack for pitch angle 0° and tip-speed ratio of 3.4

Table 4 Simulated maximum and minimum values for azimuthal angle vs. angle of attack at a pitch angle of 0° and tip-speed ratio of 3.4

Extrema	Vortex (°)	ALM (°)
Maximum	14.81	15.46 (4.4% higher)
Minimum	−10.32 (22.4% higher)	−8.43

7 Conclusions

The power extraction of a five-bladed VACT in relation to the tip-speed ratio for three blade pitch angles has been investigated at varying water speeds and tip-speed ratios. In addition, experimental data were compared with the simulations using ALM and vortex models. The experimental results for two pitch angles (0°, +3°) and simulation results for three pitch angles (−3°, 0°, +3°) indicate that the power coefficient is the highest at 0°. Since the resolution of the experimental data is quite low, one should be careful about drawing extremely strong conclusions about the measured impact of pitch angle. Thus, simulation models have been used to expand the investigated pitch angles from −3° to +3° with a step size of 1°. The simulations suggest that a pitch angle of +1° can increase the average power capture by 0.6%. The inherent difference in the two simulation models generates different predictions for the estimated power capture of the turbine and is most likely caused by the difference in the projected angle of attack during one revolution. The pitch angles can differ up to 1° and cause a difference in predicted force in the tangential direction. Both models showed numerical stability, good agreement with experimental data, and the capability to predict the performance of a studied device under different operating conditions, making the employed

models suitable for simulating VACTs.

The performance of a vertical axis marine current turbine may be slightly improved by changing the pitch angles of the blades, and the pitch angle in the positive direction increases by one degree. These results show that the impact of the pitch angle direction on the performance of a turbine differs from that of wind turbines. A negative pitch angle can increase the average power capture of a turbine by several percentages.

Funding Supported by Jgust Richert, Standup for Energy and Vattenfall, the Swedish National Infrastructure for Computing (SNIC) at NSC at Linköping University partially funded by the Swedish Research Council under Grant Nos. 2021/23-539 and 2021/5-443.

Competing interest The authors have no competing interests to declare that are relevant to the content of this article.

References

Armstrong S, Fiedler A, Tullis S (2012) Flow separation on a high Reynolds number, high solidity vertical axis wind turbine with a straight and canted blades and canted blades with fences. Renewable Energy 41: 13-22. https://doi.org/10.1016/j.renene.2011.09.002

Bachant P, Wosnik M (2015) Simulating wind and marine hydrokinetic turbines with actuator lines in rans and les. APS Meetings Abstracts id. E28.003

Bachant P, Goude A, Wosnik M (2016a) Actuator line modeling of vertical-axis turbines. arXiv: 1605.01449 https://doi.org/10.48550/arXiv.1605.01449

Bachant P, Goude A, Wosnik M (2016b) turbinesFoam: v0.0.7. Zenodo. https://doi.org/10.5281/zenodo.49422

Bahaj AS, Molland AF, Chaplin JR, Batten WMJ (2006) Power and thrust measurements of marine current turbines under various hydrodynamic flow conditions in a cavitation tunnel and a towing tank. Renewable Energy 32(3): 407-426. https://doi.org/10.1016/j.renene.2006.01.012

Chen B, Su S, Viola IM, Greated CA (2018) Numerical investigation of vertical-axis tidal turbines with sinusoidal pitching blades. Ocean Engineering 155: 75-87. https://doi.org/10.1016/j.oceaneng.2018.02.038

Day AH, Babarit A, Fontaine A, He YP, Kraskowski M, Murai M, Penesis I, Salvatore F, Shin HK (2015) Hydrodynamic modelling of marine renewable energy devices: A state of the art review. Ocean Engineering 108: 46-49. https://doi.org/10.1016/j.oceaneng.2015.05.036

Delafin PL, Nishino T, Wang L, Kolios A (2016) Effect of the number of blades and solidity on the performance of a vertical axis wind turbine. Journal of Physics: Conference Series, 753: 022033. https://doi.org/10.1088/1742-6596/753/2/022033

Dyachuk E, Rossander M, Goude A, Bernhoff H (2015a) Measurements of the aerodynamic normal forces on a 12-kW straight-bladed vertical axis wind turbine. Energies 8(8): 8482-8496. https://doi.org/10.3390/en8088482

Dyachuk E (2015b) Aerodynamics of vertical axis wind turbines: Development of simulation tools and experiments. Uppsala: Uppsala University.

Fiedler AJ (2009) Blade offset and pitch effects on a high solidity vertical axis wind turbine. Wind Engineering 33(3): 237-246. https://doi.org/10.1260/030952409789140955

Forslund J, Goude A, Thomas K (2018) Validation of a coupled electrical and hydrodynamic simulation model for vertical axis marine current energy converters. Energies 11(11): 3067. https://doi.org/10.3390/en11113067

Garrett C, Cummins P (2007) The efficiency of a turbine in a tidal channel. Journal of Fluid Mechanics 588: 243-251. https://doi.org/10.1017/S0022112007007781

Grabbe M, Lalander E, Lundin S, Leijon M (2009). A review of the tidal current energy resource in Norway. Renewable & Sustainable Energy Reviews 13(8): 1898-1909. http://dx. doi.org/10.1016/j.rser.2009.01.026

Grabbe M, Yuen K, Apelfröjd S, Leijon M (2013) Efficiency of a directly driven generator for hydrokinetic energy conversion. Advances in Mechanical Engineering 2013: Article ID 978140. http://dx.doi.org/10.1155/2013/978140

Gu Y, Zou T, Liu H, Lin Y, Ren H, Li Q (2024) Status and challenges of marine current turbines: A global review. Journal of Marine Science and Engineering 12(6): 884. https://doi.org/10.3390/jmse12060884

Kaya MN, Uzol O, Ingham D, Köse F, Buyukzeren R (2022). The aerodynamic effects of blade pitch angle on small horisontal axis wind turbines International Journal of Numerical Methods for Heat and Fluid Flow 33(1): 120-134. https://doi.org/10.1108/HFF-02-2022-0128

Kiho S, Shiono M, Suzuki K (1996) The power generation from tidal currents by darrieus turbine. Renewable Energy, 9(1-4): 1242-1245. https://doi.org/10.1016/0960-1481(96)88501-6

Khan MJ, Bhuyan G, Iqbal MT, Quaicoe JE (2009) Hydrokinetic energy conversion systems and assessment of horizontal and vertical axis turbines for river and tidal applications: A technology status review. Applied Energy 86(10): 1823-1835. https://doi.org/10.1016/j.apenergy.2009.02.017

Klimas PC, Worstell MK (1981) Effects of blade preset pitch/offset on curved-blade Darrieus vertical axis wind turbine performance. Sandia National Laboratories Reports SAND-81-1762

Li Q, Maeda T, Kamada Y, Murata J, Furukawa K, Yamamoto M (2015) Effect of number of blades on aerodynamic forces on a straight-bladed Vertical Axis Wind Turbine, Energy 90 (part 1): 784-795. https://doi.org/10.1016/j.energy.2015.07.115

Lundin S, Forslund J, Carpman N, Grabbe M, Yuen K, Apelfr¨ojd S, Goude A, Leijon M (2013) The söderfors project: experimental hydrokinetic power station deployment and first results. Proceedings of the 10th European Wave and Tidal Energy Conference, EWTEC13, Aalborg, Denmark. Uppsala: Uppsala University

Lundin S, Forslund J, Goude A, Grabbe M, Yuen K, Leijon M (2016) Experimental demonstration of performance of a vertical axis marine current turbine in a river. Journal of Renewable and Sustainable Energy 8: 064501. https://doi.org/10.1063/1.4971817

Mannion B, McCormack V, Leen AB, Nash S (2019) A CFD investigation of a variable-pitch vertical axis hydrokinetic turbine with incorporated flow acceleration. Journal of Ocean Egnineering and Marine Energy 5: 21-39. https://doi.org/10.1007/s40722-019-00130-1

Mendoza V, Goude A (2020) Validation of an actuator line and vortex model using normal forces measurements of a straight-bladed vertical axis wind turbine. Energies 13(3): 511. https://doi.org/10.3390/en13030511

Mendoza V, Bachant P, Wosnik M, Goude A (2016) Validation of an actuator line model coupled to a dynamic stall model for pitching

motions characteristic to vertical axis turbines. Journal of Physics: Conference Series 753(2): 022043. https://doi.org/10.1088/1742-6596/753/2/022043

Mendoza V, Goude A (2017) Wake flow simulation of a vertical axis wind turbine under the influence of wind shear. Journal of Physics: Conference Series, 854: 012031. https://doi.org/10.1088/1742-6596/854/1/012031

Mendoza V, Bachant P, Ferreira C, Goude A (2018a) Near-wake flow simulation of a vertical axis turbine using an actuator line model. Wind Energy 22(2): 171-188. https://doi.org/10.1002/we.2277

Mendoza V (2018b) Aerodynamic studies of vertical axis wind turbines using the actuator line model. Uppsala: Uppsala University

Miau JJ, Liang SY, Yu RM, Hu CC, Leu TS, Cheng JC, Chen SJ (2012) Design and test of a vertical-axis wind turbine with pitch control. Applied Mechanics and Materials, 225: 338-343. https://doi.org/10.4028/www.scientific.net/AMM.225.338

Paraschivoiu I, Trifu O, Saeed F (2009) H-Darrieus wind turbine with blade pitch control. International Journal of Rotating Machinery Article ID 505343. https://doi.org/10.1155/2009/505343

Rezaeiha A, Kalkman I, Blocken B (2017) Effect of pitch angle on power performance and aerodynamics of a vertical axis wind turbine. Applied Energy 197: 132-150. https://doi.org/10.1016/j.apenergy.2017.03.128

Rossander M, Dyachuk E, Apelfröjd S, Trolin K, Goude A, Bernhoff H, Eriksson S (2015) Evaluation of a blade force measurement system for a vertical axis wind turbine using load cells. Energies 8(6): 5973-5996. https://doi.org/10.3390/en8065973

Sørensen JN, Shen WZ (1999) Computation of wind turbine wakes using combined navier-Stokes/actuator-line methodology. Proceedings of the European Wind Energy Conference EWEC'99 156-159

Uihlein A, Magagna D (2016) Wave and tidal current energy–A review of the current state of research beyond technology. Renewable & Sustainable Energy Reviews 58: 1070-1081. https://doi.org/10.1016/j.rser.2015.12.284

Yuen K, Lundin S, Grabbe M, Lalander E, Goude A, Leijon M (2011) The söderfors project: construction of an experimental hydrokinetic power station. Proceedings of the 9th European Wave and Tidal Energy Conference, EWTEC11, Southampton. Uppsala: Uppsala University 1-5

Yuen K, Apelfröjd S, Leijon M (2013) Implementation of Control System for Hydro-kinetic Energy Converter. Journal of Control Science and Engineering Article ID 342949. https://doi.org/10.1155/2013/342949

Zhou Z, Scuiller F, Charpentier JF, Benbouzid M, Tang T (2014) An up-to-date review of large marine tidal current turbine technologies. In Proceedings of IEEE PEAC 2014, Piscataway: IEEE 480-484. https://doi.org/10.1109/PEAC.2014.7037903